

Insight into phonon scattering in Si nanowires through high-field hole transport: Impacts of boundary condition and comparison with bulk phonon approximation

H Tanaka, J Suda and T Kimoto

Department of Electronic Science and Engineering, Kyoto University, Kyoto, Japan

E-mail: tanaka@semicon.kuee.kyoto-u.ac.jp

Abstract. The impact of how to model phonon scattering on hole transport in Si nanowires was studied based on Boltzmann's transport equation. Boundary conditions for atomistic description of phonons in nanowires and approximation by bulk acoustic and optical phonons were analyzed in terms of their impacts on high-field hole transport. The boundary conditions for phonons influence the drift velocity and momentum relaxation time, especially at low electric field, but the energy relaxation time hardly depends on the boundary conditions. The impacts by the change of boundary conditions can be approximated by the change of the strength of acoustic phonon scattering in bulk phonon picture, though the behavior of energy relaxation and distribution function of holes can not be reproduced by bulk phonon approximation.

1. Introduction

Silicon (Si) nanowires (NWs) are a promising candidate for the channel material of future CMOS devices owing to their high electrostatic controllability [1]. To estimate their carrier transport capability, how to model phonon scattering in NWs is important. Compared with the quantum-confinement effects on carriers in NWs, which have been discussed by various authors [2, 3], the impacts of phonon confinement [4, 5] on carrier transport have not been sufficiently clarified.

In this paper, we calculated the hole transport in Si NWs by solving Boltzmann's transport equation in both low and high electric field regions, taking account of various models and boundary conditions for phonon scattering, and their impacts on hole transport were analyzed.

2. Calculation method

2.1. Model of phonon scattering

The phonon dispersion and phonon modes in NWs were computed by a valence force field (VFF) model [6], and the electron-phonon interaction was treated atomistically [7]. Here, the boundary condition (BC) for VFF phonons was varied from free to "free+4 nm" (a NW surrounded by Si with about 4-nm thickness whose outer surface has free BC), and from fixed to "fixed+4 nm". The schematic images of these BCs are presented in Fig. 1.

Approximation by bulk phonons as elastic acoustic phonon scattering and inelastic optical phonon ($\hbar\omega_{\text{op}} = 63$ meV) scattering was also used for comparison. The expression used for bulk



phonon scattering in NWs is similar to that in [8], except the substitution of atom-averaged tight-binding probability density ((probability at an atom in a unit cell)/ $N_{\text{cell}} \times 8/a_0^3$) for squared envelope function ($|\psi_n(y, z)|^2/L$), where L , N_{cell} , and a_0 are the total system length, the number of unit cells (as a NW) in L , and the lattice constant of bulk, respectively.

2.2. Model of hole transport

The valence band structure and wave functions were calculated by an $sp^3d^5s^*$ tight-binding approximation [9]. Considering the scattering rate of phonon scattering by Fermi's golden rule, the hole distribution functions under various electric fields were computed by solving the Boltzmann's transport equation. At high field, a nonlinear Boltzmann's transport equation was solved iteratively [10, 11]. The transport orientation and sidewalls of the targeted NW were $[110]/(1\bar{1}0)/(001)$, and the cross-section was a square of $1.9 \text{ nm} \times 1.9 \text{ nm}$. Hole density was fixed at 10^{17} cm^{-3} , and the temperature was assumed to be 300 K.

3. Results and discussion

3.1. Impacts of boundary conditions for phonons

The low-field phonon-limited mobility calculated with various BCs for VFF phonons is presented in Fig. 2(a). Free BC gives the lowest mobility, and fixed BC the highest, since the fixed BC pushes up the low-energy phonons to higher energy as shown in Fig. 2(b). For both BCs at the surface, surrounding Si thickness of 4 nm gives similar mobility, which means that surrounding Si thickness of 4 nm is sufficient to realize a “quasi-bulk” BC.

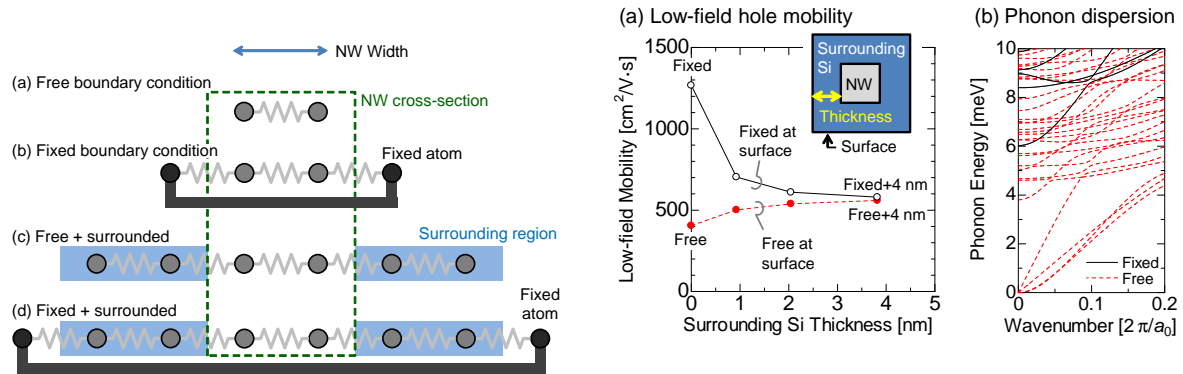


Figure 1. Schematic image of BC models for calculation of phonons in NWs by VFF.

Figure 2. (a) Low-field phonon-limited hole mobility in the Si NW with various BCs. (b) Phonon dispersions in the low-energy region by VFF for the Si NW with free and fixed BCs.

Fig. 3(a) shows the electric field F dependence of average hole drift velocity $\langle v_d \rangle$. Compared to the large difference at low field, the BC dependence of $\langle v_d \rangle$ is weaker at high field. An averaged effective mass by non-equilibrium hole distribution m_{avg} and average momentum relaxation time $\langle \tau_m \rangle$ defined as $\langle v_d \rangle = F \times e \langle \tau_m \rangle / m_{\text{avg}}$ are shown in Figs. 3(b) and (c), respectively. m_{avg} increases with F due to nonparabolicity of the valence band structure [11], and depends on BCs only weakly. The increase of m_{avg} and the decrease of $\langle \tau_m \rangle$ cause the negative differential resistance behavior of $\langle v_d \rangle$ [10, 11]. BC dependence of $\langle \tau_m \rangle$ steeply decreases at high field, as optical phonon scattering dominates, which is less affected by BCs.

To analyze the energy relaxation process, the relationship between average hole energy increase ΔE (from equilibrium) and energy relaxation time $\langle \tau_E \rangle$ defined as $1/\langle \tau_E \rangle = e \langle v_d \rangle F / \Delta E$ ($e \langle v_d \rangle F$ is the energy a hole obtains per unit time from the electric field) is depicted in Fig. 4. Fig. 4 indicates that $\langle \tau_E \rangle$ is almost independent on the BCs. This result originates from the small

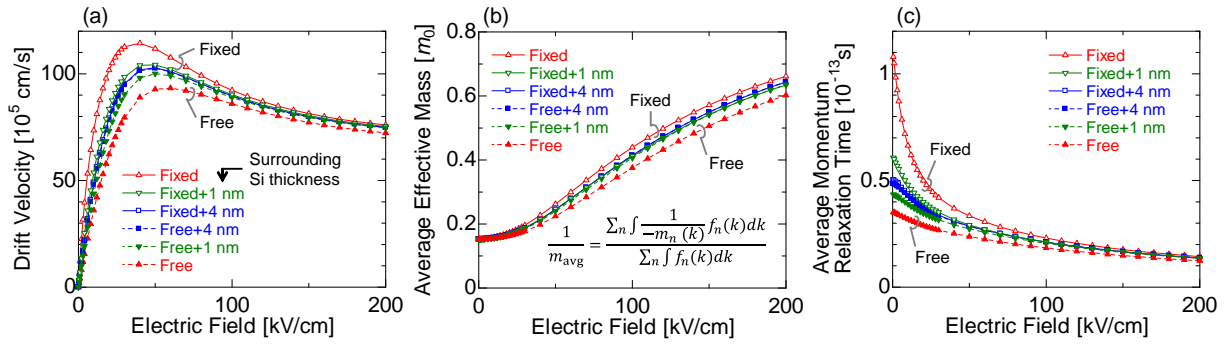


Figure 3. Field dependence of (a) average hole drift velocity $\langle v_d \rangle$, (b) average effective mass m_{avg} , and (c) average momentum relaxation time $\langle \tau_m \rangle$ in the Si NW with various BCs for VFF phonons.

impact of BCs on the phonons with large energy, which dominate energy relaxation. Thus, the smaller m_{avg} in free BC (Fig. 3(b)), which means weaker “heating” of holes, can be attributed to the smaller energy increase originating from smaller $\langle v_d \rangle$ (\propto average energy gain per unit time), not from faster energy relaxation.

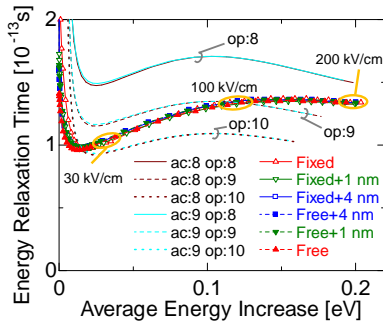


Figure 4. Energy relaxation time $\langle \tau_E \rangle$ as functions of average hole energy increase ΔE (including results by bulk phonon approximation using various D_{ac} [eV] and D_{op} [10^{10} eV/m]).

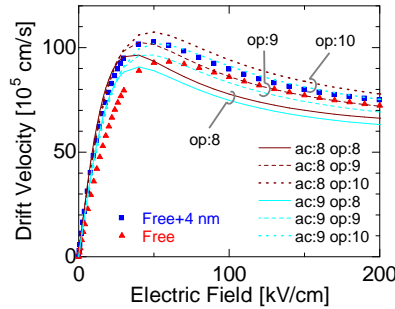


Figure 5. Field dependence of average hole drift velocity $\langle v_d \rangle$ calculated using various D_{ac} [eV] and D_{op} [10^{10} eV/m].

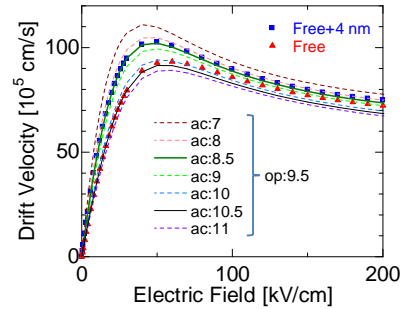


Figure 6. Field dependence of average hole drift velocity $\langle v_d \rangle$ calculated using various D_{ac} [eV] and constant D_{op} of 9.5×10^{10} eV/m.

3.2. Comparison with bulk phonon approximation

In Fig. 4, the results by bulk phonon approximation are shown, which were obtained using an acoustic phonon deformation potential (D_{ac}) of 8 or 9 eV and an optical phonon deformation potential (D_{op}) of 8, 9 or 10×10^{10} eV/m. The $\langle \tau_E \rangle$ is almost independent of D_{ac} , and this suggests that D_{op} can be fitted to $\langle \tau_E \rangle$. However, ΔE - $\langle \tau_E \rangle$ curves cannot be reproduced by any D_{op} . The trend of the larger D_{op} required to reproduce $\langle \tau_E \rangle$ by VFF phonons at smaller ΔE is explained by the contribution of acoustic phonons to energy relaxation, which is influential at small ΔE and is ignored in the bulk phonon approximation. The field dependence of $\langle v_d \rangle$ for these deformation potentials is plotted in Fig. 5 with VFF results for free and quasi-bulk (free+4 nm) BCs. Note that $\langle v_d \rangle$ at high field is larger for larger D_{op} , owing to faster energy relaxation and resulting smaller m_{avg} .

From Figs. 4 and 5, we tried to determine D_{ac} and D_{op} values that can approximate the high-field hole transport in the Si NW. Here, we assumed $D_{op} = 9.5 \times 10^{10}$ eV/m, which reproduces $\langle\tau_E\rangle$ in the 30–100 kV/cm range, and D_{ac} was fitted to $\langle v_d \rangle$. In Fig. 6, drift velocities calculated using various D_{ac} and constant D_{op} of 9.5×10^{10} eV/m are shown. D_{ac} values of 10.5 and 8.5 eV almost reproduced the F - $\langle v_d \rangle$ curves for free and quasi-bulk BCs, respectively. The factor of (10.5/8.5) means that the free BC of phonons can have an equivalent impact to about 25% increase of D_{ac} compared to quasi-bulk. This increase ratio (10.5/8.5) is close to (but smaller than) the experimentally reported increase of D_{ac} (12/9) for electrons in Si MOS interface [12] compared to bulk Si, which may validate the use of free BC to imitate the Si/oxide interface. Even though $\langle v_d \rangle$ was well reproduced around 30 kV/cm, the distribution functions are different between VFF and bulk phonons as shown in Fig. 7, resulting in different ΔE and m_{avg} .

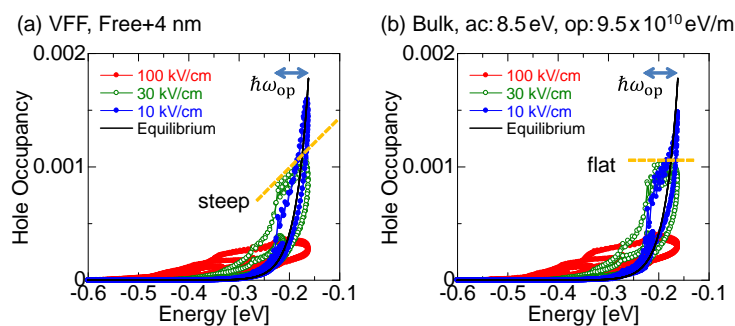


Figure 7. Calculated hole distribution functions of the Si NW under various electric fields. The case with VFF phonons with quasi-bulk BC (a) shows larger occupation near the band edge, while the results for bulk phonon approximation (b) show flatter occupation below $\hbar\omega_{op}$ from the band edge.

4. Conclusion

The boundary condition for phonons in Si NWs has strong impact on low-field hole mobility, but less at high field. The energy relaxation time is almost independent of boundary conditions. The free boundary condition in the Si NW may be described by an acoustic phonon deformation potential of about 25% larger than the quasi-bulk boundary condition. The approximation assuming elastic acoustic phonon and inelastic optical phonon scattering cannot reproduce the behavior of energy relaxation. Our results suggest that taking into account of energy relaxation by acoustic phonons in Si NWs is important to describe energy relaxation process, which is crucial in scaled MOSFETs under quasi-ballistic regime [13], and that the enhanced phonon scattering near the MOS interface may be described by a free boundary condition for phonons.

Acknowledgments

This work was supported by Japan Society for the Promotion of Science (JSPS) KAKENHI Grant Number 15J03785.

References

- [1] Park J T and Colinge J 2002 *IEEE Trans. Electron Devices* **49** 2222–9
- [2] Neophytou N, Paul A, Lundstrom M and Klimeck G 2008 *IEEE Trans. Electron Devices* **55** 1286–97
- [3] Morioka N, Yoshioka H, Suda J and Kimoto T 2011 *J. Appl. Phys.* **109** 064318
- [4] Hattori J, Uno S, Mori N and Nakazato K 2010 *Jpn. J. Appl. Phys.* **49** 04DN09
- [5] Paul A, Luisier M and Klimeck G 2011 *J. Appl. Phys.* **110** 094308
- [6] Sui Z and Herman I P 1993 *Phys. Rev. B* **48** 17938–53
- [7] Zhang W, Delerue C, Niquet Y M, Allan G and Wang E 2010 *Phys. Rev. B* **82** 115319
- [8] Ramayya E B, Vasileska D, Goodnick S M and Knezevic I 2008 *J. Appl. Phys.* **104** 063711
- [9] Niquet Y M, Rideau D, Tavernier C, Jaouen H and Blase X 2009 *Phys. Rev. B* **79** 245201
- [10] Li J, Mugny G, Niquet Y M and Delerue C 2015 *Appl. Phys. Lett.* **107** 063103
- [11] Tanaka H, Suda J and Kimoto T 2016 *Silicon Nanoelectronics Workshop (SNW2016)* pp 192–3
- [12] Takagi S, Hoyt J L, Welser J J and Gibbons J F 1996 *J. Appl. Phys.* **80** 1567–77
- [13] Datta S 2005 *Quantum Transport: Atom to Transistor* (New York: Cambridge University Press)